

1 **DSYB catalyses the key step of dimethylsulfoniopropionate biosynthesis in many**
2 **phytoplankton**

3 Andrew R. J. Curson¹, Beth T. Williams¹, Benjamin J. Pinchbeck¹, Leanne P. Sims¹, Ana
4 Bermejo Martínez¹, Peter Paolo L. Rivera¹, Deepak Kumaresan², Elena Mercadé³, Lewis G.
5 Spurgin¹, Ornella Carrión¹, Simon Moxon¹, Rose Ann Cattolico⁴, Unnikrishnan
6 Kuzhiumparambil⁵, Paul Guagliardo⁶, Peta L. Clode^{6,7}, Jean-Baptiste Raina⁵, Jonathan D.
7 Todd^{1*}

8 ¹School of Biological Sciences, University of East Anglia, Norwich Research Park, Norwich,
9 NR4 7TJ, UK. ²School of Biological Sciences and Institute for Global Food Security,
10 Queen's University Belfast, Belfast BT9 7BL, UK. ³Laboratori de Microbiologia, Facultat de
11 Farmàcia, Universitat de Barcelona, Av. Joan XXIII s/n, 08028 Barcelona, Spain.
12 ⁴Department of Biology, University of Washington, Seattle, Washington, USA. ⁵Climate
13 Change Cluster (C3), Faculty of Science, University of Technology, Sydney, NSW 2007
14 Australia. ⁶The Centre for Microscopy Characterisation and Analysis, University of Western
15 Australia, Crawley, Australia. ⁷Oceans Institute, University of Western Australia, Crawley,
16 Australia.

17 *corresponding author

18 **Dimethylsulfoniopropionate (DMSP) is a globally important organosulfur molecule, and**
19 **the major precursor for dimethyl sulfide (DMS). These compounds are important info-**
20 **chemicals, key nutrients for marine microorganisms, and are involved in global sulfur**
21 **cycling, atmospheric chemistry and cloud formation¹⁻³. DMSP production was thought**
22 **to be confined to eukaryotes, but heterotrophic bacteria can also produce DMSP, via**
23 **the pathway used by most phytoplankton⁴, and the DsyB enzyme catalysing the key step**

24 of this pathway in bacteria was recently identified⁵. However, eukaryotic phytoplankton
25 likely produce most of Earth's DMSP, yet no DMSP biosynthesis genes have been
26 identified in any such organisms. Here we identify functional *dsyB* homologues, termed
27 *DSYB*, in many phytoplankton and corals. *DSYB* is a methylthiohydroxybutyrate
28 (MTHB) methyltransferase enzyme localised in the chloroplasts and mitochondria of
29 the haptophyte *Prymnesium parvum*, and stable isotope tracking experiments support
30 these organelles as sites of DMSP synthesis. *DSYB* transcription levels increased with
31 DMSP concentrations in different phytoplankton and were indicative of intracellular
32 DMSP. The identification of the eukaryotic *DSYB* sequences, along with bacterial *dsyB*,
33 provide the first molecular tools to predict the relative contributions of eukaryotes and
34 prokaryotes to global DMSP production. Furthermore, evolutionary analysis suggests
35 that eukaryotic *DSYB* originated in bacteria and was passed to eukaryotes early in their
36 evolution.

37 Not all phytoplankton produce DMSP, and in those that do, intracellular DMSP
38 concentrations vary considerably across groups and within genera⁶. Previous studies
39 identified candidate genes^{7,8} involved in DMSP synthesis via the transamination pathway
40 (Fig. 1a), which is common to DMSP-producing bacteria⁵ and algae⁴. A proteomic study of
41 the diatom *Fragilariopsis cylindrus* identified putative DMSP synthesis enzymes⁷, including
42 the MTHB methyltransferase reaction catalysed by *DsyB* in bacteria. Another study on corals
43 identified homologues of two of the *F. cylindrus* enzymes in *Acropora millepora*, one being a
44 candidate MTHB methyltransferase⁸. None of these enzymes have been functionally ratified,
45 and the putative MTHB methyltransferases share no significant sequence similarity to *DsyB*.
46 When we cloned and expressed the *F. cylindrus* and *A. millepora* putative MTHB
47 methyltransferase genes they had no such enzyme activity (Supplementary Table 1),
48 suggesting that the identity of an algal MTHB methyltransferase was still unknown.

49 We identified homologues to the bacterial MTHB methyltransferase gene *dsyB*⁵ in available
50 genomes and/or transcriptomes of all marine prymnesiophytes; most dinoflagellates, some
51 corals, and ~20% of diatoms and Ochrophyta (Fig. 1b, Supplementary Table 2,
52 Supplementary Table 3 and Supplementary Data 1). The only dinoflagellate transcriptomes
53 lacking *dsyB* were from *Oxyrrhis marina*, a heterotroph which produces no detectable
54 DMSP^{6,9}. Furthermore, many dinoflagellates, and some haptophytes, diatoms and corals,
55 have multiple *dsyB* homologs. The grouping of these multiple homologues across the
56 phylogeny was consistent with multiple gene duplication and gene loss events over the
57 evolutionary history of eukaryotes¹⁰ (Fig. 1b, Supplementary Table 2, and Supplementary
58 Table 3). These *dsyB*-like genes, termed *DSYB*, from representatives of the corals (*Acropora*
59 *cervicornis*), diatoms (*F. cylindrus*), dinoflagellates (*Alexandrium tamarense*, *Lingulodinium*
60 *polyedrum*, *Symbiodinium microadriaticum*) and prymnesiophytes (*Chrysochromulina tobin*,
61 *Prymnesium parvum*) were cloned and shown to have MTHB methyltransferase activity, at
62 similar levels to bacterial *DsyB* from *Labrenzia* (Supplementary Table 1). These algal *DSYB*
63 enzymes fully complement bacterial *dsyB*⁻ mutants, defective in DMSP production.
64 Furthermore, enzyme assays with purified *DSYB* and DL-MTHB substrate alone showed no
65 activity but *in vitro* S-adenosyl methionine (SAM)-dependent MTHB methyltransferase
66 activity was observed when the same assays were incubated with heat-denatured *P. parvum*
67 cell lysates (Supplementary Table 4). This suggests that a co-factor(s) present in *P. parvum*
68 lysates might be required for activity. The K_M values of *DSYB* for DL-MTHB and SAM
69 were 88.2 μ M and 60.1 μ M respectively (Supplementary Table 4, Supplementary Fig. 1).
70 *DSYB* showed no detectable methyltransferase activity with other potential substrates
71 (including methionine (Met), 4-methylthio-2-oxobutyrate (MTOB) and
72 methylmercaptopropionate (MMPA); Supplementary Table 4). Thus, *DSYB* encodes the first
73 DMSP synthesis enzyme to be identified and functionally ratified from any eukaryotic algae.

74 DSYB is found across many, but by no means all, major groups of eukaryotes, and
75 eukaryotes are monophyletic in the DsyB/DSYB phylogeny, suggesting either i) that *DSYB*
76 was present in the last eukaryotic common ancestor (LECA) and has been lost across many
77 eukaryotic groups, or ii) that *dsyB* has been transferred to eukaryotes multiple times.
78 Homology and phylogenetic analyses place Alphaproteobacteria as the sister clade to the
79 eukaryotes for this gene (Fig. 1b); we note that Alphaproteobacterial genes make up a
80 significant proportion of eukaryotic genomes, due to endosymbiotic events with the ancestor
81 of mitochondria¹¹. We suggest that DMSP production originated in prokaryotes, and was
82 transferred to the eukaryotes, either via endosymbiosis at the time of mitochondrial origin, or
83 more recently via horizontal gene transfer (HGT). Interestingly, coral DSYB paralogs
84 grouped with dinoflagellate sequences from coral symbionts of the genus *Symbiodinium* (Fig.
85 1b). This is consistent with HGT between corals and their symbionts, as documented for
86 other genes¹², and suggests that DMSP production in corals may be a result of recent HGT of
87 *DSYB* from dinoflagellates. However, we cannot discount the possibility that coral DSYB
88 sequences might be contaminant sequences unintentionally extracted from their symbionts.

89 No *DSYB* homologs were identified in available transcriptomes from marine ascomycota,
90 cercozoa, chlorophyta, ciliophoran, cryptophyta, euglenozoa, glaucophyta, labyrinthista,
91 perkinsozoa, or rhodophyta (Supplementary Table 3), although some members of these taxa,
92 such as chlorophyta and rhodophyta^{9,13}, are known to produce DMSP. DSYB homologs were
93 also absent in the genomes of the DMSP-producing diatoms *Phaeodactylum tricorutum* and
94 *Thalassiosira pseudonana*¹⁴. Some marine eukaryotes lack *DSYB* simply because they do not
95 produce DMSP^{6,9}. Others may (i) have *DSYB* but not express it under the tested
96 transcriptome conditions, (ii) contain a MTHB methyltransferase isoform, or (iii) produce
97 DMSP via a different synthesis pathway¹⁵.

98 Intracellular DMSP concentrations are generally high in dinoflagellates (reported up to 3.4
99 M, but unlikely to be this high given seawater osmolarity is $\sim 1 \text{ Osm l}^{-1}$) and haptophytes (up
100 to 413 mM), but significant intra-group variance exists, with some representatives not
101 producing DMSP at detectable levels^{6,9}. Since eukaryotic DSYB enzymes had MTHB
102 methyltransferase rates similar to bacterial DsyB enzymes (Supplementary Table 1), it is
103 unlikely that variation in DsyB and DSYB amino acid sequences is responsible for the
104 differing intracellular DMSP concentrations in these organisms (Supplementary Table 1). To
105 understand this variance, we studied model DMSP-producing phytoplankton, starting with
106 *Chrysochromulina tobin* CCMP291 and *Chrysochromulina* sp. PCC307, two haptophytes
107 adapted to different salinity levels (fresh-brackish and marine waters^{16,17}, respectively). Both
108 *Chrysochromulina* strains produced very low intracellular DMSP concentrations
109 (Supplementary Table 1, Supplementary Fig. 2), which were unaffected by variation in
110 salinity and nitrogen availability, conditions that have been shown previously to affect DMSP
111 production in bacteria⁵ and phytoplankton^{7,18}. Consistent with these findings, *C. tobin*
112 CCMP291 *DSYB* was transcribed at very low levels (Supplementary Fig. 2), perhaps
113 indicating a DMSP function in these haptophytes that only requires low concentrations. Many
114 haptophytes produce high DMSP concentrations, consistent with an osmoregulatory function,
115 but this contrasts the low *C. tobin* DMSP concentrations and highlights the variability in the
116 process and requirement for a methodology to predict which phytoplankton are high and low
117 DMSP producers. Perhaps other compatible solutes, possibly sugars or amino acids, are the
118 major osmolytes in CCMP291 and PCC307. Consistent with this, the osmolyte glycine
119 betaine ($551 \pm 6 \text{ nmol}$) was present in ~ 10 -fold higher amounts than DMSP ($52 \pm 6 \text{ nmol}$) in
120 CCMP291.

121 Next, we investigated DMSP production in six *Prymnesium* strains, from brackish/marine
122 sources, and found they had similar intracellular DMSP concentrations, which were much

123 higher than those for *C. tobin* (Supplementary Fig 2). *P. parvum* CCAP946/6 *DSYB*
124 transcription was also higher than that for *C. tobin DSYB* under standard conditions
125 (Supplementary Fig 2). Interestingly, *DSYB* transcription, *DSYB* protein levels and DMSP
126 concentration in *P. parvum* were all enhanced by increased salinity but unaffected by other
127 environmental conditions, including nitrogen availability or temperature (Supplementary Fig.
128 2; Supplementary Fig. 3). Increased salinity enhances DMSP production in many
129 phytoplankton, notably *P. parvum*, where DMSP is thought to be a significant osmolyte¹⁹.
130 Our findings, and those of Dickson and Kirst¹⁹, are consistent with DMSP playing an
131 osmoregulatory role in this haptophyte. However, *dsyB* transcription and DMSP production is
132 regulated by salinity in bacteria, yet no detrimental effect on growth was observed in a
133 bacterial *dsyB* mutant when grown in saline conditions⁵. Thus, increased *DSYB* expression
134 and DMSP production with raised salinity does not necessarily indicate a major role for
135 DMSP in osmoprotection.

136 *P. parvum DSYB* protein was concentrated to the chloroplasts and mitochondria (Fig. 2;
137 Supplementary Fig. 4). We propose these organelles as sites of DMSP synthesis in *P. parvum*
138 and perhaps other eukaryotic phytoplankton. Although DMSP production in mitochondria
139 has not been reported, DMSP is produced in the chloroplasts of the higher plant *Wollastonia*,
140 albeit using a different pathway²⁰. Based on *in silico* sequence analysis (see Methods), *DSYB*
141 from *P. parvum* and some other phytoplankton are predicted to be targeted to the
142 mitochondria and/or chloroplasts (Supplementary Table 5). However, chromophyte algae,
143 such as haptophytes and diatoms, have complex plastids²¹, which may render such *in silico*
144 predictions less reliable.

145 Nanoscale secondary-ion mass spectrometry (NanoSIMS), with a cryopreservation method
146 previously shown to preserve cytosolic DMSP²², was used to identify potential sub-cellular

147 sites of DMSP production and storage in *P. parvum* through tracking $^{34}\text{SO}_4$ uptake. After 48 h
148 incubation, $\sim 23.2\% \pm 0.2$ of the *P. parvum* intracellular DMSP pool was labelled with ^{34}S
149 (^{34}S -DMSP; Supplementary Fig. 5). Within the cells, the ^{34}S appeared to be localized in sub-
150 cellular compartments, with increasing levels appearing over time in the chloroplasts ($^{34}\text{S}/^{32}\text{S}$:
151 3.4 ± 0.17 after 48 h) and in submicrometer hotspots ($^{34}\text{S}/^{32}\text{S}$: 3.1 ± 0.15 after 48 h) (Fig. 3).
152 Given the size and location of these hotspots, they are likely to be mitochondria or small lipid
153 vesicles (Fig. 3). Although many sulfur compounds are present in algal cells, DMSP
154 represents more than 50% of the total organosulfur compounds in marine phytoplankton²³
155 and it is expected to account for a significant fraction of the ^{34}S signal detected by
156 NanoSIMS. However, it cannot be discounted that the increased ^{34}S content in the chloroplast
157 could be due to transport of sulfur and subsequent assimilation via plastid-located enzymes,
158 such as ATP sulfurylase, APS reductase and sulfite reductase. Nonetheless, the simultaneous
159 increase in ^{34}S in the chloroplasts and potentially mitochondria supports our hypothesis that
160 these organelles are indeed sites of DMSP synthesis and storage in *P. parvum* and likely other
161 phytoplankton. Given the role of these organelles in energy production, it is perhaps not
162 surprising that DMSP production, an energy-demanding process²⁴, may occur at these sites.
163 With DMSP being far less concentrated in the cytosol, it is less likely that its primary
164 function in *P. parvum* is as a typical cytosolic osmolyte, but it may be a key osmolyte in the
165 chloroplasts and/or mitochondria, as proposed in *Wollastonia* chloroplasts²⁰. Also,
166 considering reactive oxygen species (ROS) are generated in the mitochondria and
167 chloroplasts, and that DMSP is an effective scavenger of ROS²⁵, the production of DMSP in
168 these organelles is in line with its putative role in oxidative stress protection^{24,25}.

169 Diatoms are thought to produce the lowest intracellular DMSP levels (typically $< 50\text{ mM}$)⁹.
170 We studied DMSP production in the polar ice diatom *Fragilariopsis cylindrus*, one of the few
171 diatoms with a functional *DSYB* (Supplementary Table 2), finding that, under standard

172 conditions, intracellular DMSP levels and *DSYB* transcription were relatively low, when
173 compared to (e.g.) *P. parvum* (Supplementary Fig. 2). However, consistent with work in
174 other diatoms¹⁸, both *F. cylindrus* DMSP production and *DSYB* transcription increased with
175 nitrogen limitation and increased salinity (Supplementary Fig. 2). The latter supports a role
176 for DMSP in osmoregulation and salinity-induced oxidative stress protection in *F. cylindrus*,
177 as suggested by Lyon et al.⁷. *DSYB* was not detected as one of the salinity-induced proteins
178 in Lyon et al.⁷, despite using the same salinity conditions for our experiments, reflecting the
179 nature of 2D gel electrophoresis studies, whereby not all proteins are identified.

180 Given the trend of intracellular DMSP concentration increasing with *DSYB* transcription, we
181 studied *Symbiodinium microadriaticum* CCMP2467, a dinoflagellate from a genus producing
182 high DMSP concentrations⁶. *S. microadriaticum* gave the highest intracellular DMSP (282
183 mM) and cumulative *DSYB* transcription of the tested phytoplankton (Supplementary Fig. 2).
184 Similarly, available transcriptomic data showed that high DMSP-producing dinoflagellate
185 and haptophyte phytoplankton (see above) had the highest average *DSYB* transcription, which
186 was ~3 and 8-fold higher, respectively, than that in diatoms (Supplementary Table 2).
187 Transcriptomic data was also congruent with high variability in intracellular DMSP levels
188 within dinoflagellates and haptophytes^{6,9}. While additional factors, such as *DSYB* protein
189 levels, DMSP excretion, DMSP catabolism and cell volume, will affect an organism's
190 intracellular DMSP concentration, the data presented here on a small number of
191 phytoplankton supports the hypothesis that *DSYB* transcription is a reasonably good indicator
192 of DMSP concentration. Some *DSYB*-containing phytoplankton may also contain MTHB
193 methyltransferase isoform enzymes or utilise other DMSP synthesis pathways, in which case
194 such predictions may be inaccurate. Further work is required to substantiate this hypothesis.

195 The prominence of environmental DMSP-producing bacteria and eukaryotes was examined
196 in the ocean microbial reference gene catalogue (OM-RGC) metagenomic dataset, generated
197 from samples fractionated to $< 3 \mu\text{m}^26$ (Supplementary Table 6 and Supplementary Fig. 6).
198 *dsyB* genes were predicted to be present in 0.35% of total bacteria in these samples. For
199 comparison, DMSP lyase genes (*dddD*, *dddL*, *dddK*, *dddP*, *dddQ*, *dddW*, *dddY* and *AlmaI*)²⁷,
200 were also used. The *dsyB* gene was more abundant than *dddL*, *dddW*, *dddY*, and the algal
201 DMSP lyase *AlmaI*, but was less abundant than *dddD*, *dddK*, *dddP* and *dddQ* in the OM-
202 RGC dataset. Despite only 3% of the OM-RGC microorganisms likely being eukaryotes²⁶,
203 *DSYB* genes were detected and were ~25-fold less abundant than bacterial *dsyB*. Since no
204 *DSYB* sequences have been identified in bacteria, we conclude that picoeukaryotes in these
205 samples contain *DSYB* and thus, the genetic potential to make DMSP. The production of
206 DMSP by *DSYB*-containing picoeukaryotes could contribute, along with DMSP-producing
207 bacteria, to the DMSP measured from particles $< 2 \mu\text{m}$ in size in seawater samples²⁸.

208 We also investigated the occurrence of *dsyB* and *DSYB* in marine metatranscriptomes
209 (Supplementary Table 7). *dsyB* transcripts were detected in all tested *Tara* oceans
210 metatranscriptomic datasets apportioned to marine bacteria (Supplementary Table 8 and
211 Supplementary Fig. 6). *dsyB* transcript abundance (normalised to total sequence numbers)
212 was similar to *dddD* and greater than *dddL*, *dddW*, *dddY* and *AlmaI*, but was far less than
213 *dddK*, *dddP* and *dddQ*. Although these datasets do not consider phytoplankton $> 3 \mu\text{m}$, *DSYB*
214 transcripts, likely from picoeukaryotes, were detected at levels only 3-fold lower than the
215 bacterial *dsyB* gene, again suggesting that these smaller eukaryotes, like bacteria, should be
216 considered as potentially significant DMSP producers (Supplementary Table 8).

217 We also analysed the North Pacific Ocean metatranscriptomes (GeoMICS) which used
218 appropriate fractionation methods for bacteria and larger phytoplankton²⁹. As expected,

219 eukaryotic *DSYB* transcript numbers were higher than those of bacterial *dsyB* in all of the 2-
220 53 μm fractions, which should contain relatively more phytoplankton than bacteria, and the
221 opposite was true in most of the 0.2-2 μm fractions, which should have relatively more
222 bacteria but not contain the larger phytoplankton (Supplementary Table 9). Analysing data
223 from both the large and small size fractions at different sites allowed us to gauge the relative
224 total transcript numbers of *DSYB* and *dsyB* in these samples, as well as those of the DMSP
225 lyase genes. Prokaryotic *dsyB* transcripts (normalised to the recovery of the internal standard)
226 were more abundant than those for the bacterial DMSP lyase genes *dddK*, *dddL*, *dddQ*, *dddY*
227 and *dddW*, 3-fold less than *dddP* and *Alma1* and 27-fold less than *dddD* (Supplementary
228 Table 9). Eukaryotic *DSYB* transcripts were slightly less abundant than those for the
229 eukaryotic DMSP lyase (*Alma1*), but, were ~2-fold more abundant than those for bacterial
230 *dsyB*. With similar DsyB and DSYB enzyme rates (Supplementary Table 1), this
231 metatranscriptomic data suggests that eukaryotic phytoplankton may be the major
232 contributors to DMSP production via the DsyB/DSYB pathway in these samples. However,
233 direct extrapolation from these data to predict eukaryotic versus bacterial DMSP production
234 (via DsyB/DSYB) is not likely accurate since other factors, such as DsyB/DSYB protein
235 stability or the differing expression and activities of other enzymes in the pathway, may also
236 affect DMSP production. Nonetheless, *dsyB* and *DSYB* sequences provide invaluable tools
237 for future, in-depth studies to investigate the relative contribution of bacterial and algal
238 DMSP production in varied marine environments. Molecular studies are also required to
239 identify DMSP synthesis genes in DMSP-producing organisms which lack *dsyB* or *DSYB*.

240

241 **Methods**

242 **Media and general growth of algae and bacteria**

243 *Prymnesium parvum* CCAP941/1A, *Prymnesium parvum* CCAP941/6, *Prymnesium parvum*
244 CCAP946/1B, *Prymnesium parvum* CCAP946/1D, *Prymnesium parvum* CCAP946/6,
245 *Prymnesium patelliferum* CCAP946/4, *Chrysochromulina* sp. PCC307 and *Symbiodinium*
246 *microadriaticum* CCMP2467 were grown in F/2³⁰ medium made with ESAW artificial
247 seawater³¹ and without any added Na₂SiO₃. Axenic *Fragilariopsis cylindrus* CCMP1102 was
248 supplied by Mock et al.³² and grown in F/2 medium made with ESAW artificial seawater at 4
249 °C with a light intensity of 120 μE m⁻² s⁻¹ and constant illumination. *Chrysochromulina tobin*
250 CCMP291 was grown in the proprietary medium RAC-5³³. All algal cultures (except *F.*
251 *cylindrus*) were grown at 22 °C with a light intensity of 120 μE m⁻² s⁻¹ and a light dark cycle
252 of 16 h light/8 h dark, unless otherwise stated. Where necessary, media for algal growth were
253 modified according to the requirements of the experimental conditions being tested. Where
254 strains were not already known to be axenic, cultures were treated with multiple rounds of
255 antibiotic treatment prior to experiments. Test cultures with and without antibiotic treatments
256 showed no significant difference in total DMSP in samples. For *P. parvum* CCAP946/6, and
257 *Chrysochromulina* sp. PCC307 cultures, streptomycin (400 μg ml⁻¹), chloramphenicol (50 μg
258 ml⁻¹), gentamicin (20 μg ml⁻¹) and ampicillin (100 μg ml⁻¹) were added, and for *S.*
259 *microadriaticum* cultures, streptomycin (100 μg ml⁻¹) and neomycin (100 μg ml⁻¹) were
260 added. *E. coli* was grown in LB³⁴ complete medium at 37 °C. *R. leguminosarum* was grown
261 in TY³⁵ complete medium or Y³⁵ minimal medium (with 10 mM succinate as carbon source
262 and 10 mM NH₄Cl as nitrogen source) at 28 °C. *L. aggregata* J571 was grown in YTSS³⁶
263 complete medium or MBM³⁷ minimal medium (with 10 mM succinate as carbon source and
264 10 mM NH₄Cl as nitrogen source) at 30 °C. Where necessary, antibiotics were added to
265 bacterial cultures at the following concentrations: streptomycin (400 μg ml⁻¹), kanamycin (20
266 μg ml⁻¹), spectinomycin (200 μg ml⁻¹), gentamicin (20 μg ml⁻¹), ampicillin (100 μg ml⁻¹).
267 Strains used in this study are listed in Supplementary Table 10.

268

269 **Staining with 4',6-diamidino-2-phenylindole (DAPI)**

270 The absence of bacterial contamination was confirmed by epifluorescence microscopy of
271 culture samples stained with DAPI³⁸. Briefly, 13 ml of culture was removed and fixed with
272 765 μ l paraformaldehyde, then 130 μ l of DAPI stain (1 mg ml⁻¹ in H₂O) was added and
273 samples were stored in the dark at 4 °C for 16 h. After staining, 3 ml of the stained cells were
274 removed and filtered onto a Whatman Nuclepore track-etched membrane (25 mm, 0.2 μ m,
275 polycarbonate). To prepare slides, one drop of immersion oil was added onto the slide then
276 the sample filter was placed on the oil and another drop of immersion oil was added onto the
277 filter. A cover slip was then placed on top of the filter and pressed down with forceps to
278 remove air bubbles. The slide was then tilted and left on absorbent paper towel to allow any
279 excess oil to drain/wick away. Slides were examined using an Olympus BX40 microscope
280 equipped with an Olympus Camedia C-7070 digital camera.

281

282 **General *in vivo* and *in vitro* genetic manipulations**

283 Plasmids (Supplementary Table 10) were transferred to *E. coli* by transformation, and
284 *Rhizobium leguminosarum* J391 or *Labrenzia aggregata* J571 by conjugation in a triparental
285 mating using the helper plasmid pRK2013³⁹. Routine restriction digestions and ligations for
286 cloning were performed essentially as in Downie et al.⁴⁰. The oligonucleotide primers used
287 for molecular cloning were synthesised by Eurofins Genomics and are detailed in
288 Supplementary Table 11. Sequencing of plasmids and PCR products was performed by
289 Eurofins Genomics.

290 The *DSYB* gene from *P. parvum* CCAP946/6 was PCR-amplified from cDNA and cloned
291 into the IPTG-inducible wide host range expression plasmid pRK415⁴¹. All other *DSYB*
292 genes were synthesised by Eurofins Genomics, from sequences codon-optimised (using
293 Invitrogen GeneArt) for expression in *E. coli*, in the vector pEX-K4 (Eurofins Genomics).
294 The synthesised genes were then subcloned into pLMB509⁴², a taurine-inducible plasmid for
295 the expression of genes in *Rhizobium* and *Labrenzia*, using *NdeI* and *BamHI* or *EcoRI*
296 restriction enzymes. All plasmid clones are described in Supplementary Table 10.

297

298 **MTHB methyltransferase (MMT) assays**

299 To measure MMT activity from pLMB509 clones expressing the *dsyB* or *DSYB* gene in *R.*
300 *leguminosarum* J391, cultures were grown (in triplicate) overnight in TY complete medium,
301 1 ml of culture was centrifuged at 20,000g for 2 min, resuspended in the same volume of Y
302 medium and then diluted 1:100 into 5 ml Y with 10 mM taurine (to induce expression,
303 Sigma-Aldrich, T0625), 0.5 mM DL-MTHB (Sigma-Aldrich, 55875), 0.1 mM L-methionine
304 and gentamycin, and incubated at 28 °C for 60 h before sampling for gas chromatography
305 (GC) analysis (see ‘Quantification of DMS and DMSP by gas chromatography’) to determine
306 the amount of DMSP product.

307 To measure MMT activity from pLMB509 clones expressing the *DSYB* gene in the *L.*
308 *aggregata dsyB* mutant strain J571, cultures were grown (in triplicate) overnight in YTSS
309 complete medium. Following incubation, 1 ml of culture was then centrifuged at 20,000g for
310 2 min, resuspended in the same volume of MBM medium and then diluted 1:50 into 5 ml
311 MBM with 10 mM taurine (to induce expression, Sigma-Aldrich), rifampicin and
312 gentamycin, and incubated at 30 °C for 24 h. Samples were taken for GC analysis and
313 determining protein concentration (t = 0 h timepoint). DL-MTHB (0.5 mM) and L-

314 methionine (0.1 mM) were then added as substrates to the remaining cultures and these were
315 incubated for 4 h at 30 °C before sampling for GC and protein again (t = 4 h timepoint), with
316 activity calculated based on the difference in measured DMSP product between t=0 h and t=4
317 h.

318 To measure DMSP in *Rhizobium* or *Labrenzia* assay mixtures, 200 µl of culture was added to
319 a 2 ml glass serum vial then 100 µl 10 M NaOH was added and vials were crimped
320 immediately, incubated at 22 °C for 24 h and monitored by GC assay (see ‘Quantification of
321 DMS and DMSP by gas chromatography’). DsyB/DSYB activity is expressed as pmol DMSP
322 mg protein⁻¹ min⁻¹, assuming that all the DMSP is derived from DMSHB through DDC
323 activity. LC-MS analysis shows no detectable DMSHB in *Rhizobium* or *Labrenzia*
324 expressing DsyB/DSYB, presumably due its conversion to DMSP by DDC activity, so
325 DMSP production is used as a proxy for DsyB activity. Protein concentrations were
326 determined using the Bradford method (BioRad). Control assays of *Rhizobium* or *Labrenzia*
327 J571 containing pLMB509 were carried out, as above, and gave no detectable DsyB/DSYB
328 activity.

329

330 **Growth of algae under non-standard conditions**

331 For all *P. parvum*, *F. cylindrus* and *C. tobin* cultures described here, all samples were taken
332 in mid exponential phase growth before growth rates started to decline (checked by
333 continuing to monitor growth following sampling). To measure DMSP production or
334 *DSYB/DSYB* expression in *P. parvum* CCAP946/6 under different conditions, the growth
335 conditions or F/2 medium were modified as follows. Standard growth conditions were a
336 temperature of 22 °C, light intensity of 120 µE m⁻² s⁻¹, salinity of 35 practical salinity units
337 (PSU) and nitrogen concentration of 882 µM. For increased or decreased salinity, the amount

338 of salts added to the artificial seawater were adjusted to give a salinity of 50 or 10 PSU
339 respectively. For reduced nitrogen concentration cultures, the F/2 medium contained 88.2 μ M
340 (10% of standard F/2). For changes in temperature, cultures were grown at 15 °C or 28 °C.
341 To measure the effect of increased salinity and nitrogen limitation in *F. cylindrus*
342 CCMP1102, this strain was grown in F/2 medium with increased salts in the artificial
343 seawater (to 70 PSU) or reduced nitrogen (88.2 μ M, 10% of standard F/2). To measure the
344 effect of increased salinity and nitrogen limitation in *C. tobin* CCMP291, this strain was
345 grown in F/2 medium with sea salts added to the RAC-5 medium (to 5 PSU) or reduced
346 nitrogen (85 μ M, 10% of standard RAC-5).

347

348 **Sampling methods**

349 To measure growth of algal cultures, samples were removed, diluted (dependent on level of
350 growth) in artificial seawater and cell counting was done using a Multisizer 3 Coulter counter
351 (Beckman Coulter). The effect of stress on photosystem II was determined by measuring
352 Fv/Fm values using a Phyto-Pam phytoplankton analyzer (Heinz Walz, Germany). To obtain
353 samples for DMSP quantification by GC or liquid chromatography-mass spectrometry (LC-
354 MS), 25 ml of culture was filtered onto 47 mm GF/F glass microfiber filters (Fisher
355 Scientific, UK) using a Welch WOB-L 2534 vacuum pump, and filters were then blotted on
356 paper towel to remove excess liquid and stored at -80 °C in 2 ml centrifuge tubes for
357 particulate DMSP (DMSPp) measurement. To obtain samples for RNA, 50 ml of culture was
358 filtered onto 47 mm 1.2 μ m RTTP polycarbonate filters (Fisher Scientific, UK) and filters
359 were stored in 2 ml centrifuge tubes at -80 °C. To obtain samples for protein for Western
360 blotting, 50 ml of culture was centrifuged at 600g for 10 min in a 50 ml centrifuge tube, the
361 supernatant was decanted and cells were transferred in the residual liquid to a 2 ml centrifuge

362 tube and centrifuged at 600g for 5 mins. All residual liquid was then aspirated and the
363 pelleted cells were stored at -80 °C.

364

365 **Quantification of DMS and DMSP by GC**

366 All GC assays involved measurement of headspace DMS, either directly produced or via
367 alkaline lysis of DMSP or DMSHB, using a flame photometric detector (Agilent 7890A GC
368 fitted with a 7693 autosampler) and a HP-INNOWax 30 m x 0.320 mm capillary column
369 (Agilent Technologies J&W Scientific). All GC measurements were performed using 2 ml
370 glass serum vials containing 0.3 ml liquid samples and sealed with PTFE/rubber crimp caps.
371 Quantification of DMSP from algal samples filtered on GF/F glass microfiber filters (see
372 ‘Sampling methods’) was performed following methanol extraction. Filters were folded,
373 placed in a 2 ml centrifuge tube and 1 ml 100% methanol was added. Samples were stored for
374 24 h at -20 °C to allow the extraction of cellular metabolites, then 200 µl of the methanol
375 extract was added to a 2 ml vial, 100 µl 10 M NaOH was added, vials were crimped
376 immediately, incubated at 22 °C for 24 h in the dark and monitored by GC. Control samples
377 in which DMSP standards were added to algal sample filters prior to methanol extraction
378 showed that all standard was recovered following our extraction and measurement procedure.
379 Calibration curves were produced by alkaline lysis of DMSP standards in water (for
380 *Rhizobium/Labrenzia* MMT assays) or 100% methanol (for algal methanol extracts), or DL-
381 DMSHB (chemically synthesised as in Curson et al.⁵) standards in water with heating at 80
382 °C for 10 mins (to release DMS from DMSHB) (for assays with purified DSYB protein). The
383 detection limit for headspace DMS from DMSP was 0.015 nmol in water and 0.15 nmol in
384 methanol, and from DMSHB was 0.3 nmol in water.

385

386 **Quantification of DMSP by LC-MS**

387 LC-MS was used to confirm that phytoplankton were producing DMSP and at similar levels
388 to that shown by GC, ruling out the possibility that DMS detected by GC was due to some
389 other compound and not DMSP. Samples were extracted as follows: GF/F filters of
390 phytoplankton (see 'Sampling methods') were resuspended in 1 ml of 80% LC-MS grade
391 acetonitrile (extraction solvent), and mixed by pipetting and vortexing for 2 min. The
392 resulting mixture was transferred into a fresh 2 ml Eppendorf tube. For a second round of
393 extraction, another 1 ml of the extraction solvent was then added and mixed as previously
394 described. Then the filters were centrifuged at 18,000g for 10 min and the supernatant was
395 collected, giving a total volume of 2 ml of the collected supernatant. The collected
396 supernatant was then centrifuged at 18,000g for 10 min and 1.5 ml of the supernatant was
397 collected for LC-MS analysis. To extract the metabolites from *Chrysochromulina* sp.
398 CCMP291, 20 ml of sample was centrifuged at 600g for 10 min and the cell pellet was
399 resuspended in a total volume of 0.7 ml of the extraction solvent and mixed by pipetting and
400 vortexing for 2 min. Samples were then centrifuged at 18,000g for 10 min and 0.5 ml of the
401 supernatant was collected for LC-MS analysis.

402 LC-MS was carried out using a Shimadzu Ultra High Performance Liquid Chromatography
403 (UHPLC) system formed by a Nexera X2 LC-30AD Pump, a Nexera X2 SIL-30AC
404 Autosampler, a Prominence CTO-20AC Column oven, and a Prominence SPD-M20A Diode
405 array detector; and a Shimadzu LCMS-2020 Single Quadrupole Liquid Chromatograph Mass
406 Spectrometer. Samples were analysed in hydrophilic interaction chromatography (HILIC)
407 mode using a Phenomenex Luna NH2 column (100 x 2 mm with a particle size of 3 µm) at
408 pH 3.75. Mass spectrometry spray chamber conditions were capillary voltage 1.25 kV, oven

409 temperature 30 °C, desolvation temperature 250 °C and nebulising gas flow 1.50 L min⁻¹.
410 Solvent A is 5% acetonitrile + 95% 5 mM ammonium formate in water. Solvent B is 95%
411 acetonitrile + 5% 100 mM ammonium formate in water. Flow rate was 0.6 ml min⁻¹ and
412 gradient (% solvent A/B) was t = 1 min, 100% B; t = 3.5 min, 70% B; t = 4.1 min, 58% B; t =
413 4.6 min, 50% B; t = 6.5 min, 100% B; t = 10 min, 100% B. The injection volume was 15 µl.
414 All samples were analysed immediately after being extracted. The targeted mass transition
415 corresponded to [M+H]⁺ of DMSP (m/z 135) and of glycine betaine (m/z 118) in positive
416 mode. A calibration curve was performed for quantification of DMSP and glycine betaine
417 using a mixture of DMSP and glycine betaine standards in the extraction solvent.

418

419 **Reverse transcription quantitative PCR (RT-qPCR)**

420 For each culture, RNA was extracted as follows: 1 ml Trizol reagent (Sigma-Aldrich),
421 prewarmed at 65 °C, was added directly to the frozen phytoplankton filter (see ‘Sampling
422 methods’), followed by 600 mg of < 106 µm glass beads (Sigma-Aldrich). Cells were
423 disrupted using an MP FastPrep®-24 instrument set at maximum speed for 3 x 30 seconds.
424 Following a 5 min recovery time at 22 °C, samples were centrifuged at 13,000g, 4 °C, for 2
425 min. The supernatant was transferred to a 2 ml screwcap tube containing 1 ml 95% ethanol
426 and RNA was extracted using a Direct-zol™ RNA MiniPrep kit (Zymo Research, R2050),
427 according to the manufacturer’s specifications.

428 Genomic DNA was removed by treating samples with TURBO DNA-free™ DNase
429 (Ambion®) according to the manufacturer’s protocol. The quantity and quality of the RNA
430 was determined by a NanoDrop 2000 UV-Vis Spectrophotometer (Thermo Scientific) using 1
431 µl of sample.

432 Reverse transcription of 1 µg DNA-free RNA was achieved using the QuantiTect® Reverse
433 Transcription Kit (Qiagen). Primers (Supplementary Table 11) were designed, using
434 Primer3Plus⁴³, to amplify ~130 bp region, with an optimum melting temperature of 60 °C.
435 Melting temperature difference between primers in a pair was 2 °C and GC content was kept
436 between 40-60%.

437 Quantitative PCR was performed with a C1000 Thermal cycler equipped with a CFX96 Real-
438 time PCR detection system (BioRad), using a SensiFAST™ SYBR® Hi-ROX Kit (Bioline)
439 as per the manufacturer's instructions for a 3-step cycling programme. Reactions (20 µl)
440 contained 50 ng cDNA and a final concentration of 400 nM of each primer, with a 60 °C
441 annealing temperature. Gene expression for each condition was performed upon
442 three biological replicates, each with three technical replicates. Control DNA consisted of
443 pGEMT-Easy (Promega) containing the fragment created by the RT-qPCR primer pair for
444 each gene tested (made through PCR on synthesised cDNA, cloning in *E. coli* 803 and
445 purifying via a Miniprep Kit [Qiagen]).

446 For each condition and gene, the cycle threshold (Ct) values of the technical and biological
447 replicates were averaged and manually detected outliers were excluded from further analysis.
448 Standard curves of control DNA were calculated from 3 points of 1:10 serial dilutions,
449 starting with 0.01 ng, to absolutely quantify the *DSYB* transcripts for comparison between
450 organisms⁴⁴. For an individual organism, relative *DSYB* expression was normalised to the β-
451 actin housekeeping gene, and calculated using the $2^{-\Delta\Delta CT}$ method⁴⁵ to observe changes in
452 response to various conditions.

453

454 **Analysis of *DSYB* expression by Western blotting**

455 A polyclonal rabbit IgG was designed against *P. parvum* DSYB using the
456 OptimumAntigen™ software (GenScript Ltd.). The purified IgG was used as a primary
457 antibody in Western blotting and immunogold labelling (see ‘DSYB immunogold labelling’).
458 The specificity of this antibody was ensured by Western blot analysis of DSYB expressed in
459 the heterologous host *R. leguminosarum* J391. J391 strains containing pBIO2275 (positive
460 control) and pRK415 with no cloned insert (negative control) were grown overnight in TY
461 medium with 0.5 mM IPTG. Proteins were extracted by harvesting 1 ml culture, resuspending
462 cell pellet in 200 µl 20 mM HEPES, 150 mM NaCl, pH 7.5 and disrupting with an ultrasonic
463 processor (Cole Palmer) for 2 x 10 s cycles on ice. Cell debris was separated by
464 centrifugation at 18,000g for 10 mins, following which the supernatant was mixed with SDS
465 sample buffer and incubated at 95 °C for 5 min, before resolution on a 15 % (v/v) acrylamide
466 gel.

467 The specificity of the anti-DSYB antibody was additionally tested on *P. parvum* 946/6, where
468 protein samples were prepared from cell pellets (see ‘Sampling methods’) as for *R.*
469 *leguminosarum*, without the removal of cell debris. Cell lysate containing 5.5 µg protein was
470 mixed with SDS sample buffer and heat-treated at 95 °C for 20 min, before resolution on a 15
471 % (v/v) acrylamide gel.

472 Following SDS-PAGE, proteins were transferred to a PVDF membrane (Amersham
473 Hybond™-P, GE Healthcare) by semi-dry Western blot as outlined by Mahmood and Yang⁴⁶.
474 After 1 hour blocking with 5 % (w/v) skimmed milk powder in TBS (20 mM Tris, 150 mM
475 NaCl, pH 7.5), the anti-DSYB antibody was added at a final concentration of 0.386 µg ml⁻¹.
476 Specific interactions were left to form overnight at 4 °C, before the membrane was washed 4
477 x 10 min with TBST (TBS + 0.1 % (v/v) Tween 20). TBST (20 ml) was added with 3 µl anti-
478 rabbit IgG-alkaline phosphatase at 1 mg ml⁻¹ (Sigma). Following 1 h incubation, the

479 membrane was washed as before with two 10 min TBS washes. Colorimetric detection with
480 NBT/BCIP (Thermo Fisher) was used to detect the target protein as per the manufacturer's
481 instructions. All SDS-PAGE gels were run with Bio-Rad Precision Plus Dual Colour protein
482 size standards and stained with Coomassie using InstantBlue Protein stain (Expedeon).

483

484 **Purification of DSYB and *in vitro* catalytic assays**

485 A 1.1 kb fragment of DNA containing the coding region of *Chrysochromulina tobin* DSYB
486 was cloned into pET16b as an *NdeI/EcoRI* restriction fragment, downstream of a 10-histidine
487 coding sequence, and transformed into *E. coli* BL21 DE3 (New England BioLabs), for
488 protein purification. Batch cultures were grown aerobically in LB medium at 37 °C until
489 reaching an OD₆₀₀ value of ~0.6 and were then supplemented with 0.2 mM IPTG and
490 incubated at 28 °C overnight to induce recombinant protein expression. Cells were harvested
491 at 5,000g for 20 min and resuspended in buffer A (20 mM HEPES, 150 mM NaCl, 25 mM
492 imidazole, pH 7.5). The mixture was supplemented with protease inhibitor (Roche cOmplete
493 Tablets, Mini EDTA-free, EASYpack (cat. no. 04 693 159 001)), lysed via sonication and
494 separated at 15,000g, 4 °C for 30 min.

495 DSYB was purified via an immobilized metal affinity chromatography (IMAC, HiTrap
496 Chelating HP, GE Healthcare) column charged with NiSO₄ and equilibrated with buffer A.
497 All steps were performed at 24 °C with a flow rate of 1 ml min⁻¹. Soluble cell lysate was
498 loaded and washed through with 4 column volumes of buffer A. Bound protein was eluted
499 into 1 ml fractions using a stepped gradient of 25 to 150 mM imidazole, applied for 2 column
500 volumes each. Fractions were visualised via SDS-PAGE analysis (Supplementary Fig. 7) and
501 those containing DSYB were pooled and dialysed at 4 °C overnight against 20 mM HEPES,
502 150 mM NaCl, pH 7.5.

503 *P. parvum* lysate was prepared by centrifuging 100 ml of culture at a late exponential phase
504 for 10 min at 2,500g. The pellet was washed with 20 mM HEPES, 150 mM NaCl, pH 7.5 and
505 resuspended in 2 ml buffer supplemented with EDTA-free protease inhibitor (Roche
506 cOmplete Tablets, Mini EDTA-free, *EASY*pack (cat. no. 04 693 159 001)). Cells were
507 sonicated 3 x 10 s to lyse, with a 50 s recovery time at 4 °C. Resulting lysate was heat-treated
508 at 80 °C for 10 min to denature proteins (ensuring no activity from native DSYB protein) and
509 centrifuged for 2 min 14 000g. Supernatant was removed to a fresh Eppendorf tube and used
510 for downstream catalytic assays.

511 DSYB MTHB methyltransferase activity was monitored by performing *in vitro* enzyme
512 assays in 400 µl reactions with 50 µl *P. parvum* lysate and 350 µl purified DSYB (~0.1 mg
513 ml⁻¹) or buffer. All enzyme substrates were added to a final concentration of 1 mM and
514 reactions were incubated at 28 °C for 30 mins. Following this, 800 µl of finely ground
515 charcoal (38 mg ml⁻¹ in 0.1 M acetic acid) was added to the samples and mixed to remove
516 SAM. Samples were centrifuged for 10 mins, 14,000g and the supernatant was retained. For
517 GC analysis, 200 µl of the supernatant was added to a 2 ml vial, 100 µl 10 M NaOH was
518 added, vials were crimped immediately, then heated at 80 °C for 10 minutes (to release DMS
519 from DMSHB) and finally incubated at 22 °C for 24 h in the dark. These samples were
520 subsequently used for quantification of DMSHB by GC analysis as described earlier and
521 activities are reported as nmol DMSHB mg protein⁻¹ min⁻¹. DMS produced from background
522 DMSHB/DMSP present in the *P. parvum* lysate was subtracted from the reported activities.

523

524 **DSYB immunogold labelling**

525 Cells from *P. parvum* 946/6 were cryoimmobilized using a Leica EMPACT High-Pressure
526 Freezer (Leica Microsystems), freeze-substituted in an EM AFS (Leica Microsystems) and
527 embedded in Lowicryl HM20 resin (EMS, Hatfield, USA) as in Perez-Cruz et al.⁴⁷. Gold

528 grids containing Lowicryl HM20 ultrathin sections were immunolabeled with a specific
529 primary antibody to *P. parvum* DSYB (polyclonal rabbit IgG, GenScript), whose stock
530 concentration was 0.550 mg ml⁻¹ and this was diluted 1:15000. Secondary antibody was an
531 IgM anti-rabbit coupled to 12 nm diameter colloidal gold particles (Jackson) diluted 1:30. As
532 controls, pre-immune rabbit serum was used as primary antibody, or the gold-conjugated
533 secondary antibody was used without the primary antibody. Sections were observed in a
534 Tecnai Spirit microscope (FEI, Eindhoven, The Netherlands) at 120 kV.

535

536 ***Prymnesium* growth and experimental conditions for NanoSIMS**

537 *P. parvum* were grown as previously described in F/2 medium (35 PSU)³⁰. Sodium sulfate
538 (Na₂SO₄, 25 mM) was used as the sole sulfur source, with either ³⁴S (90% ³⁴S (Sigma-
539 Aldrich, USA; hereafter called ³⁴S-F/2) or natural abundance of ³²S (95% ³²S, 0.7% ³³S, 4.2%
540 ³⁴S; hereafter called ^{nat}S-F/2). Consequently, the composition of the both the trace metals and
541 vitamin complement had to be slightly modified (with Riboflavin replacing the sulfur-
542 containing Biotin and Thiamine)²². *P. parvum* cells in late exponential phase (grown in ^{nat}S-
543 F/2) were centrifuged at low speed (1,000g) for 5 mins, rinsed with ³⁴S-F/2 (to remove
544 potential leftover ^{nat}S) and transferred in ³⁴S-F/2, whereas a batch incubated only in ^{nat}S-F/2
545 acted as a control. Culture were sampled at four time-points: directly after the medium
546 exchange, and after 6 hrs, 24 hrs and 48 hrs. At each timepoint, cultures were sampled for
547 NanoSIMS, mass-spectrometry and cell counts (see below).

548

549 **Flow cytometry for NanoSIMS samples**

550 Cells were enumerated in triplicate *via* flow cytometry (BD Accuri C6, Becton Dickinson,
551 USA). For each sample, forward scatter (FSC), side scatter (SSC), and red (chlorophyll)

552 fluorescence were recorded. The samples were analysed at a flow rate of 35 $\mu\text{l min}^{-1}$.
553 *Prymnesium* populations were characterized according to SSC and chlorophyll fluorescence
554 and cell abundances were calculated by running a standardized volume of sample (50 μl).

555

556 **Sample collection for mass spectrometry (NanoSIMS)**

557 At each time point, 1 ml of culture was centrifuged at low speed (1,000g) for 5 mins, the
558 supernatant was discarded and the cell pellet was extracted with 80% methanol, sonicated on
559 ice for 30 mins and dried.

560 Dried extracts were reconstituted in methanol to perform LC-MRM-MS analysis. The LC-
561 MS system consisted of an Agilent 1290 series LC interfaced to an Agilent G6490A QQQ
562 mass spectrometer (Agilent, Santa Clara, CA, USA). The MS was equipped with an
563 electrospray ionization source and was controlled by Mass Hunter workstation (version B07)
564 software. A HILIC column (Luna Phenomenex, 150 \times 3 mm, 5 μm , 300 Å) was used for the
565 on-line separations, at a flow rate of 1 ml min^{-1} . The gradient used consisted of a 95 %
566 solvent B (Acetonitrile, 0.1% formic acid), followed by a 2 min linear gradient to 40% A
567 (Milli Q, 0.1 % formic acid), then a 10 min linear gradient to 90% A, and returning to initial
568 conditions at 12.25 min. The injection volume was 2 μl . The MS acquisition parameters
569 were: positive ion mode; capillary voltage, 3000 V; gas flow 12 l min^{-1} ; nebulizer gas, 20
570 p.s.i.; sheath gas flow rate 7 l/ min^{-1} at a temperature of 250 °C. Acquisition was done in
571 MRM mode with transitions m/z 135- > 63 and m/z 137- > 65 for quantifying $^{32}\text{DMSP}$ and
572 $^{34}\text{DMSP}$ respectively. The collision energy was optimised as 10 eV to detect the highest
573 possible intensity.

574

575 **Sample collection and preparation for NanoSIMS**

576 Samples for NanoSIMS were collected and processed following the method described by
577 Raina et al.²². Briefly, samples were snap-frozen, and embedded following by a water-free
578 embedding procedure to effectively prevent the loss of highly soluble compounds such as
579 DMSP from the samples. This method does retain elements in solution by effectively
580 replacing the ‘solution’ with resin, without displacing the ions and osmolytes. *Prymnesium*
581 cultures (20 µl) were dropped onto Thermanox strips (Thermo Fisher Scientific, Waltham,
582 USA, 4×18 mm) and placed in humidified chambers. After 20 min, the cells settled onto the
583 strips and the excess medium was carefully removed with filter paper. The strips were then
584 immediately snap-frozen by immersion into liquid nitrogen slush²². Samples were stored in
585 liquid nitrogen until required. Frozen samples for NanoSIMS were freeze-substituted in
586 anhydrous 10% acrolein in diethyl ether, and warmed progressively to room temperature over
587 three weeks in an EM AFS2 automatic freeze-substitution unit (Leica Microsystems, Wetzlar,
588 Germany) as described recently in step-by-step detail by Kilburn and Clode⁴⁸. The samples
589 were subsequently infiltrated and embedded in anhydrous Araldite 502 resin, after which the
590 Thermanox strip was removed and the sample re-embedded and stored in a desiccator. No
591 sulfur was present in processing or resin components. Resin sections (1 mm thick) of
592 embedded *Prymnesium* cells were cut dry using a Diatome-Histo diamond knife on an EM
593 UC6 Ultramicrotome (Leica Microsystems, Wetzlar, Germany), mounted on a silicon wafer
594 and coated with 10 nm of gold.

595

596 **NanoSIMS analysis**

597 The NanoSIMS-50L (Cameca, Gennevilliers, France) at the Centre for Microscopy,
598 Characterisation and Analysis (CMCA) at the University of Western Australia was used for
599 all subsequent analyses. The NanoSIMS-50L allows simultaneous collection and counting of

600 seven isotopic species, which enables the determination of $^{34}\text{S}/^{32}\text{S}$ ratio. Enrichments of the
601 rare isotope ^{34}S was confirmed by an increase in the sulfur ($^{34}\text{S}/^{32}\text{S}$) ratio above natural
602 abundance values recorded in controls (0.0438). NanoSIMS analysis was undertaken by
603 rastering a 2.5 pA Cs^+ beam (~ 100 nm diameter) across defined $20\ \mu\text{m}^2$ sample areas
604 (256×256 pixels), with a dwell time of 30 ms per pixel. The isotope ratio values are
605 represented hereafter using a colour-coded transform (hue saturation intensity (HSI)) showing
606 natural abundance levels in blue, and grading to high enrichment in pink. Images were
607 processed and analysed using Fiji (<http://fiji.sc/Fiji>)⁴⁹ with the Open-MIMS plug-in
608 (<http://nrims.harvard.edu/software>). All images were dead-time corrected⁵⁰. Ratio data were
609 tested for QSA (quasi-simultaneous arrivals) by applying different beta values from 0.5 to
610 162. No differences in the data were observed, indicating that the secondary ion count rates
611 were too low to be affected by QSA. Quantitative data were extracted from the mass images
612 through manually drawn regions of interest, at T0 (whole cells $n = 7$, hotspot $n = 10$,
613 chloroplasts $n = 3$), at T6 (whole cells $n = 14$, hotspot $n = 10$, chloroplasts $n = 6$), at T24
614 (whole cells $n = 12$, hotspot $n = 10$, chloroplasts $n = 9$), and at T48 (whole cells $n = 6$, hotspot
615 $n = 10$, chloroplasts $n = 4$).

616

617 **Statistics**

618 Statistical methods for RT-qPCR are described in the relevant section above. All
619 measurements for DMSP production or DSYB/DsyB enzyme activity (in algal strains or
620 enzyme assays) are based on the mean of at least three biological replicates per
621 strain/condition tested, with all experiments performed at least twice. To identify statistically
622 significant differences between standard and experimental conditions in Supplementary Fig.
623 2, a single-tailed independent Student's t -test ($P < 0.05$) was applied to the data, using R⁵¹.

624

625 **Identification of DSYB proteins in eukaryotes**

626 BLASTP and TBLASTN searches⁵² were used to identify homologues of the *Labrenzia* DsyB
627 protein in available eukaryotic genomes and/or transcriptome assemblies at NCBI or JGI.

628 Any eukaryotic DsyB-like proteins (E values $\leq 1e^{-30}$), were aligned to ratified bacterial DsyB
629 sequences and to non-functional DsyB-like proteins, e.g., in *Streptomyces varsoviensis*, see
630 below. Representative DsyB-like proteins, more similar to DsyB than to non-functional *S.*
631 *varsoviensis* DsyB-like proteins, were cloned and assayed for MMT activity (as above).

632 Ratified eukaryotic DSYB peptide sequences were used in BLASTP searches of 119
633 eukaryotic transcriptomes (with replicates) downloaded from the Marine Microbial
634 Eukaryote Transcriptome Sequencing Project (MMETSP)⁵³ via the sequencing repositories
635 iMicrobe (<http://imicrobe.us/project/view/104>) and ENA (European Nucleotide Archive)⁵⁴.
636 Of these, 45 contained at least one hit to DSYB (E values $\geq 1e^{-30}$) (Supplementary Table 3).
637 Each potential DsyB/DSYB sequence was manually curated by BLASTP analysis against the
638 RefSeq database and discounted as a true DSYB sequence if the top hits were not to ratified
639 DSYB sequences detailed in Fig. 1b. DSYB sequences identified from iMicrobe
640 transcriptomes were aligned to ratified DsyB and DSYB sequences and included in the
641 evolutionary analysis (Fig. 1b). All DsyB and DSYB protein sequences identified from
642 genomes or transcriptomes are listed in Supplementary Data 1. Kallisto⁵⁵ was used to
643 quantify transcript abundances. Firstly, Kallisto indexes were created for the combined
644 nucleotide assemblies of each organism. Next, Kallisto quant was used to obtain Transcripts
645 Per kilobase Million (TPM) expression values for all datasets using the relevant reference
646 transcriptome index for that organism. Nucleotide sequences corresponding to the DSYB hits
647 were obtained using TBLASTN, and the CAMNT ID number was used to identify the TPM

648 values for each *DSYB* read, giving an estimate of gene expression for organisms grown in
649 standard conditions.

650

651 **Phylogenetic analysis of DSYB and DsyB proteins**

652 All prokaryotic DsyB and eukaryotic DSYB amino acid sequences were aligned in
653 MAFFT^{56,57} version 7 using default settings, then visually checked. Prior to phylogeny
654 construction, model selection was carried out and the best supported model of sequence
655 evolution based on the Bayesian Information Criterion (BIC)⁵⁸ was selected for phylogeny
656 construction (the LG+I+G4 model⁵⁹). A maximum likelihood phylogeny was then
657 constructed using IQ-TREE⁶⁰ version 1.5.3, implemented in the W-IQ-TREE web interface⁶¹,
658 with 1000 ultrafast bootstrap replicates⁶² used to assess node support. The resulting tree was
659 rooted using a non-DsyB methyltransferase sequence from *Streptomyces varsoviensis*⁵, and
660 was formatted for publication using the ggtree package⁶³ in R⁵¹.

661

662 **Analysis of DSYB sequences for localisation signals**

663 Searches for localisation signals in the DSYB protein sequences used the prediction software
664 packages SignalP 4.1 (<http://www.cbs.dtu.dk/services/SignalP/>), TargetP 1.1
665 (<http://www.cbs.dtu.dk/services/TargetP/>) and ChloroP 1.1
666 (<http://www.cbs.dtu.dk/services/ChloroP/>).

667

668 **Analysis of marine metagenomes and metatranscriptomes**

669 Hidden Markov Model (HMM)-based searches for *dsyB* and *DSYB* homologs in metagenome
670 and metatranscriptome datasets were performed as described in⁶⁴ using HMMER tools
671 (version 3.1, <http://hmmer.janelia.org/>). The DsyB/DSYB protein sequences, shown in Fig.
672 1b, and ratified DddD⁶⁵⁻⁶⁸, DddK⁶⁹, DddL⁷⁰, DddP⁷¹, DddQ⁷², DddY⁷³, DddW⁷⁴ and Alma1⁷⁵
673 sequences were used as training sequences to create the HMM profiles. Profile HMM-based
674 searches eliminate the bias associated with single sequence BLAST queries⁷⁶. HMM profiles
675 for the *recA* gene were downloaded from the functional gene pipeline and repository
676 (FunGene⁷⁷). The *Ruegeria pomeroyi* DddW⁷⁴ sequence was used to search metagenome and
677 metatranscriptome datasets via BLASTP⁵² since it is the only ratified DddW. HMM and
678 BLASTP searches were performed against peptide sequences predicted from OM-RGC
679 database assemblies (Supplementary Table 6) and all hits with an e-value cut-off of $1e^{-30}$
680 were retrieved. In the case of metatranscriptome datasets (*Tara* Oceans and GeOMICs
681 metatranscriptomes), homologs with an e-value cutoff of $1e^{-5}$ were retrieved. Each potential
682 DsyB/DSYB sequence retrieved from the analysis of metagenomes and metatranscriptomes
683 was manually curated by BLASTP analysis against the RefSeq database and discounted as a
684 true DsyB sequence if the top hits were not to DsyB or DSYB sequences detailed in Fig. 1b.
685 If the top hits were to eukaryotic DSYB then the gene was counted as a true DSYB sequence,
686 and vice versa for bacterial DsyB. Each of the DddD, DddK, DddL, DddP, DddQ, DddW,
687 DddY and Alma1 peptide sequences retrieved were aligned to curated reference sequences
688 using hmalign and an approximate maximum likelihood tree was constructed using
689 FastTree⁷⁸ v2.1. Putative Ddd or Alma1 peptide sequences not aligning most closely to
690 functional Ddd or Alma1 enzymes were removed. To estimate the percentage of bacteria
691 containing *dsyB*, the number of unique hits to DsyB in metagenomes was normalised to the
692 number of RecA sequences. Retrieved DsyB/DSYB homolog sequences were aligned to the
693 training sequences using the *dsyB* HMM alignment and this was used to construct an

694 approximately maximum likelihood phylogenetic tree inferred using FastTree⁷⁸ v2.1. The
695 resulting tree (Supplementary Fig. 6) was visualised and annotated using the Interactive Tree
696 Of Life (iTOL)⁷⁹ version 3.2.4.

697 The GeoMICS metatranscriptome database²⁹ generated from North Pacific Ocean samples
698 offered an opportunity to compare prokaryotic and eukaryotic gene expression. Sequences
699 from both the 0.2 μm – 2 μm and 2 μm – 53 μm filtrate fractions for sites P1 and P6 (those
700 samples that had duplicates) were obtained from NCBI (Accession: PRJNA272345)
701 (Supplementary Table 7). Sequences were trimmed using TrimGalore (default parameters,
702 paired-end mode, https://www.bioinformatics.babraham.ac.uk/projects/trim_galore/) and
703 overlapping paired-end reads were joined using PandaSeq⁸⁰. To create peptide databases, the
704 joined reads were translated using the translate function in Sean Eddy's squid package
705 (<http://selab.janelia.org/software.html>) to generate all ORFs above 20 amino acids in length.
706 The resulting peptide sequences were used to retrieve *dsyB* and *DSYB* sequences using HMM
707 searches and BLASTP (as above). Read numbers for *dsyB/DSYB* were normalised to the read
708 numbers of internal standard²⁹ recovered in each sample by dividing the number of reads by
709 the internal standard number and multiplying by 100. Normalised reads from the same site
710 and fraction were averaged (Supplementary Table 9) and ratios of *dsyB/DSYB* calculated.

711

712 **Data availability statement** The datasets analysed during the current study are available in
713 the iMicrobe (<https://www.imicrobe.us/#/projects/104>), European Nucleotide Archive
714 (<https://www.ebi.ac.uk/ena>), NCBI (<https://www.ncbi.nlm.nih.gov/>) and Ocean Microbiome
715 (<http://ocean-microbiome.embl.de/companion.html>) repositories or are available within the
716 paper in Methods section ‘Analysis of marine metagenomes and metatranscriptomes’ and in

717 Supplementary Tables 7, 8 and 9. All data that support the findings of this study are available
718 from the corresponding author upon reasonable request.

719 **References**

- 720 1. Nevitt, G. A. The neuroecology of dimethyl sulfide: a global-climate regulator turned
721 marine infochemical. *Integr. Comp. Biol.* **51**, 819–825 (2011).
- 722 2. Sievert, S. M., Kiene, R. P. & Schulz-Vogt, H. N. The sulfur cycle. *Oceanography* **20**,
723 117–123 (2007).
- 724 3. Curson, A. R., Todd, J. D., Sullivan, M. J. & Johnston, A. W. Catabolism of
725 dimethylsulphonioacetate: microorganisms, enzymes and genes. *Nat. Rev.*
726 *Microbiol.* **9**, 849–859 (2011).
- 727 4. Summers, P. S. *et al.* Identification and stereospecificity of the first three enzymes of
728 3-dimethylsulfonylpropionate biosynthesis in a chlorophyte alga. *Plant Physiol.* **116**,
729 369–378 (1998).
- 730 5. Curson, A. R. *et al.* Dimethylsulfonylpropionate biosynthesis in marine bacteria and
731 identification of the key gene in this process. *Nat. Microbiol.* **2**, 17009 (2017).
- 732 6. Caruana, A. M. N. & Malin, G. The variability in DMSP content and DMSP lyase
733 activity in marine dinoflagellates. *Prog. Oceanogr.* **120**, 410–424 (2014).
- 734 7. Lyon, B. R., Lee, P. A., Bennett, J. M., DiTullio, G. R. & Janech, M. G. Proteomic
735 analysis of a sea-ice diatom: salinity acclimation provides new insight into the
736 dimethylsulfonylpropionate production pathway. *Plant Physiol.* **157**, 1926–1941
737 (2011).
- 738 8. Raina, J. B. *et al.* DMSP biosynthesis by an animal and its role in coral thermal stress
739 response. *Nature* **502**, 677–680 (2013).

- 740 9. Keller, M. D., Bellows, W. K. & Guillard, R. R. L. *Dimethyl sulfide production in*
741 *marine phytoplankton. Biogenic sulfur in the environment* (American Chemical
742 Society, 1989).
- 743 10. Nei, M. & Rooney, A. P. Concerted and birth-and-death evolution of multigene
744 families. *Annu. Rev. Genet.* **39**, 121–152 (2005).
- 745 11. Ku, C. *et al.* Endosymbiotic origin and differential loss of eukaryotic genes. *Nature*
746 **524**, 427–432 (2015).
- 747 12. Baumgarten, S. *et al.* The genome of *Aiptasia*, a sea anemone model for coral
748 symbiosis. *Proc. Natl. Acad. Sci. U. S. A.* **112**, 11893–11898 (2015).
- 749 13. Van Alstyne, K. L. & Puglisi, M. P. DMSP in marine macroalgae and
750 macroinvertebrates: Distribution, function, and ecological impacts. *Aquat. Sci.* **69**,
751 394–402 (2007).
- 752 14. Spielmeier, A. & Pohnert, G. Influence of temperature and elevated carbon dioxide on
753 the production of dimethylsulfoniopropionate and glycine betaine by marine
754 phytoplankton. *Mar. Environ. Res.* **73**, 62–69 (2012).
- 755 15. Dickschat, J. S., Rabe, P. & Citron, C. A. The chemical biology of
756 dimethylsulfoniopropionate. *Org. Biomol. Chem.* **13**, 1954–1968 (2015).
- 757 16. Hovde, B. T. *et al.* Genome sequence and transcriptome analyses of *Chrysochromulina*
758 *tobin*: metabolic tools for enhanced algal fitness in the prominent order Prymnesiales
759 (Haptophyceae). *PLoS Genet.* **11**, (2015).
- 760 17. Jones, H. L. J., Leadbeater, B. S. C. & Green, J. C. Mixotrophy in marine species of
761 *Chrysochromulina* (Prymnesiophyceae) - ingestion and digestion of a small green
762 flagellate. *J. Mar. Biol. Assoc. United Kingdom* **73**, 283–296 (1993).

- 763 18. Kettles, N. L., Kopriva, S. & Malin, G. Insights into the regulation of DMSP synthesis
764 in the diatom *Thalassiosira pseudonana* through APR activity, proteomics and gene
765 expression analyses on cells acclimating to changes in salinity, light and nitrogen.
766 *PLoS One* **9**, (2014).
- 767 19. Dickson, D. M. J. & Kirst, G. O. Osmotic adjustment in marine eukaryotic algae - the
768 role of inorganic-ions, quaternary ammonium, tertiary sulfonium and carbohydrate
769 solutes .2. Prasinophytes and Haptophytes. *New Phytol.* **106**, 657–666 (1987).
- 770 20. Trossat, C. *et al.* Salinity promotes accumulation of 3-dimethylsulfoniopropionate and
771 its precursor S-methylmethionine in chloroplasts. *Plant Physiol.* **116**, 165–171 (1998).
- 772 21. Gruber, A. *et al.* Protein targeting into complex diatom plastids: functional
773 characterisation of a specific targeting motif. *Plant Mol. Biol.* **64**, 519–530 (2007).
- 774 22. Raina, J. B. *et al.* Subcellular tracking reveals the location of
775 dimethylsulfoniopropionate in microalgae and visualises its uptake by marine bacteria.
776 *Elife* **6**, (2017).
- 777 23. Matrai, P. A. & Keller, M. D. Total organic sulfur and dimethylsulfoniopropionate in
778 marine phytoplankton: intracellular variations. *Mar. Biol.* **119**, 61–68 (1994).
- 779 24. Stefels, J. Physiological aspects of the production and conversion of DMSP in marine
780 algae and higher plants. *J. Sea Res.* **43**, 183–197 (2000).
- 781 25. Sunda, W., Kieber, D. J., Kiene, R. P. & Huntsman, S. An antioxidant function for
782 DMSP and DMS in marine algae. *Nature* **418**, 317–320 (2002).
- 783 26. Sunagawa, S. *et al.* Structure and function of the global ocean microbiome. *Science*
784 (80-). **348**, (2015).
- 785 27. Johnston, A. W. B., Green, R. T. & Todd, J. D. Enzymatic breakage of

- 786 dimethylsulfoniopropionate - a signature molecule for life at sea. *Curr. Opin. Chem.*
787 *Biol.* **31**, 58–65 (2016).
- 788 28. Belviso, S. *et al.* Size distribution of dimethylsulfoniopropionate (DMSP) in areas of
789 the tropical northeastern Atlantic Ocean and the Mediterranean Sea. *Mar. Chem.* **44**,
790 55–71 (1993).
- 791 29. Amin, S. A. *et al.* Interaction and signalling between a cosmopolitan phytoplankton
792 and associated bacteria. *Nature* **522**, 98–101 (2015).
- 793 30. Guillard, R. R. L. Culture of phytoplankton for feeding marine invertebrates. in
794 *Culture of Marine Invertebrate Animals* (ed. Smith Chanley, M. H., W. L.) 26–60
795 (Plenum Press, 1975).
- 796 31. Berges, J. A., Franklin, D. J. & Harrison, P. J. Evolution of an artificial seawater
797 medium: Improvements in enriched seawater, artificial water over the last two
798 decades. *J. Phycol.* **37**, 1138–1145 (2001).
- 799 32. Mock, T. *et al.* Evolutionary genomics of the cold-adapted diatom *Fragilariopsis*
800 *cylindrus*. *Nature* **541**, 536–540 (2017).
- 801 33. Fixen, K. R. *et al.* Genome sequences of eight bacterial species found in coculture with
802 the haptophyte *Chrysochromulina tobin*. *Genome Announc.* **4**, e01162-16 (2016).
- 803 34. Sambrook, J., Fritsch, E. F., Maniatis, T. & Nolan, C. *Molecular cloning, a laboratory*
804 *manual.* **3**, (Cold Spring Harbor Laboratory Press, 1989).
- 805 35. Beringer, J. E. R factor transfer in *Rhizobium leguminosarum*. *J. Gen. Microbiol.* **84**,
806 188–198 (1974).
- 807 36. Gonzalez, J. M., Whitman, W. B., Hodson, R. E. & Moran, M. A. Identifying
808 numerically abundant culturable bacteria from complex communities: An example

- 809 from a lignin enrichment culture. *Appl. Environ. Microbiol.* **62**, 4433–4440 (1996).
- 810 37. Baumann, P. & Baumann, L. *The marine Gram-negative eubacteria: genera*
811 *Photobacterium, Beneckeella, Alteromonas, Pseudomonas and Alcaligenes. In The*
812 *Prokaryotes* (Springer-Verlag, 1981).
- 813 38. Porter, K. G. & Feig, Y. S. The use of DAPI for identifying and counting aquatic
814 microflora. *Limnol. Oceanogr.* **25**, 943–948 (1980).
- 815 39. Figsur, D. H. & Helinski, D. R. Replication of an origin-containing derivative of
816 plasmid Rk2 dependent on a plasmid function provided in trans. *Proc. Natl. Acad. Sci.*
817 *U. S. A.* **76**, 1648–1652 (1979).
- 818 40. Downie, J. A. *et al.* Cloned nodulation genes of *Rhizobium leguminosarum* determine
819 host range specificity. *Mol. Gen. Genet.* **190**, 359–365 (1983).
- 820 41. Keen, N. T., Tamaki, S., Kobayashi, D. & Trollinger, D. Improved broad-host-range
821 plasmids for DNA cloning in Gram-negative bacteria. *Gene* **70**, 191–197 (1988).
- 822 42. Tett, A. J., Rudder, S. J., Bourdes, A., Karunakaran, R. & Poole, P. S. Regulatable
823 vectors for environmental gene expression in alphaproteobacteria. *Appl. Environ.*
824 *Microbiol.* **78**, 7137–7140 (2012).
- 825 43. Untergasser, A. *et al.* Primer3-new capabilities and interfaces. *Nucleic Acids Res.* **40**,
826 (2012).
- 827 44. Heid, C. A., Stevens, J., Livak, K. J. & Williams, P. M. Real time quantitative PCR.
828 *Genome Res.* **6**, 986–994 (1996).
- 829 45. Livak, K. J. & Schmittgen, T. D. Analysis of relative gene expression data using real-
830 time quantitative PCR and the 2^(-Delta Delta C) method. *Methods* **25**, 402–408
831 (2001).

- 832 46. Mahmood, T. & Yang, P. C. Western blot: technique, theory, and trouble shooting. *N.*
833 *Am. J. Med. Sci.* **4**, 429–434 (2012).
- 834 47. Perez-Cruz, C. *et al.* New type of outer membrane vesicle produced by the Gram-
835 negative bacterium *Shewanella vesiculosa* M7T: implications for DNA content. *Appl.*
836 *Environ. Microbiol.* **79**, 1874–1881 (2013).
- 837 48. Kilburn, M. R. & Clode, P. L. Electron microscopy. in (Humana Press, 2014).
- 838 49. Schindelin, J. *et al.* Fiji: An open source platform for biological image analysis. *Nat.*
839 *Methods* **9**, 676–682 (2012).
- 840 50. Hillion, F., Kilburn, M. R., Hoppe, P., Messenger, S. & Webers, P. K. The effect of
841 QSA on S, C, O and Si isotopic ratio measurements. *Geochim. Cosmochim. Acta* **72**,
842 A377 (2008).
- 843 51. Team, R. D. C. R: *A Language and Environment for Statistical Computing*. (R
844 Foundation for Statistical Computing, 2008).
- 845 52. Altschul, S. F. *et al.* Gapped BLAST and PSI-BLAST: a new generation of protein
846 database search programs. *Nucleic Acids Res.* **25**, 3389–3402 (1997).
- 847 53. Keeling, P. J. *et al.* The marine microbial eukaryote transcriptome sequencing project
848 (MMETSP): Illuminating the functional diversity of eukaryotic life in the oceans
849 through transcriptome sequencing. *PLoS Biol.* **12**, (2014).
- 850 54. Toribio, A. L. *et al.* European nucleotide archive in 2016. *Nucleic Acids Res.* **45**, D32–
851 D36 (2017).
- 852 55. Bray, N. L., Pimentel, H., Melsted, P. & Pachter, L. Near-optimal probabilistic RNA-
853 seq quantification. *Nat. Biotechnol.* **34**, 525–527 (2016).
- 854 56. Katoh, K., Misawa, K., Kuma, K. & Miyata, T. MAFFT: a novel method for rapid

- 855 multiple sequence alignment based on fast Fourier transform. *Nucleic Acids Res.* **30**,
856 3059–3066 (2002).
- 857 57. Katoh, K. & Standley, D. M. MAFFT multiple sequence alignment software version 7:
858 Improvements in performance and usability. *Mol. Biol. Evol.* **30**, 772–780 (2013).
- 859 58. Schwarz, G. Estimating dimension of a model. *Ann. Stat.* **6**, 461–464 (1978).
- 860 59. Le, S. Q. & Gascuel, O. An improved general amino acid replacement matrix. *Mol.*
861 *Biol. Evol.* **25**, 1307–1320 (2008).
- 862 60. Nguyen, L. T., Schmidt, H. A., von Haeseler, A. & Minh, B. Q. IQ-TREE: A fast and
863 effective stochastic algorithm for estimating maximum-likelihood phylogenies. *Mol.*
864 *Biol. Evol.* **32**, 268–274 (2015).
- 865 61. Trifinopoulos, J., Nguyen, L. T., von Haeseler, A. & Minh, B. Q. W-IQ-TREE: a fast
866 online phylogenetic tool for maximum likelihood analysis. *Nucleic Acids Res.* **44**,
867 W232–W235 (2016).
- 868 62. Minh, B. Q., Nguyen, M. A. T. & von Haeseler, A. Ultrafast approximation for
869 phylogenetic bootstrap. *Mol. Biol. Evol.* **30**, 1188–1195 (2013).
- 870 63. Yu, G. C., Smith, D. K., Zhu, H. C., Guan, Y. & Lam, T. T. Y. GGTREE: an R
871 package for visualization and annotation of phylogenetic trees with their covariates
872 and other associated data. *Methods Ecol. Evol.* **8**, 28–36 (2017).
- 873 64. Esson, K. C. *et al.* Alpha and gammaproteobacterial methanotrophs co-dominate the
874 active methane oxidizing communities in an acidic boreal peat bog. *Appl. Environ.*
875 *Microbiol.* **82**, 2363–2371 (2016).
- 876 65. Todd, J. D. *et al.* Structural and regulatory genes required to make the gas dimethyl
877 sulfide in bacteria. *Science (80-.).* **315**, 666–669 (2007).

- 878 66. Todd, J. D. *et al.* Molecular dissection of bacterial acrylate catabolism--unexpected
879 links with dimethylsulfoniopropionate catabolism and dimethyl sulfide production.
880 *Environ. Microbiol.* **12**, 327–343 (2010).
- 881 67. Curson, A. R. J., Sullivan, M. J., Todd, J. D. & Johnston, A. W. B. Identification of
882 genes for dimethyl sulfide production in bacteria in the gut of Atlantic Herring (*Clupea*
883 *harengus*). *ISME J.* **4**, 144–146 (2010).
- 884 68. Curson, A. R. J., Fowler, E. K., Dickens, S., Johnston, A. W. B. & Todd, J. D.
885 Multiple DMSP lyases in the gamma-proteobacterium *Oceanimonas doudoroffii*.
886 *Biogeochemistry* **110**, 109–119 (2012).
- 887 69. Sun, J. *et al.* The abundant marine bacterium *Pelagibacter* simultaneously catabolizes
888 dimethylsulfoniopropionate to the gases dimethyl sulfide and methanethiol. *Nat.*
889 *Microbiol.* **1**, (2016).
- 890 70. Curson, A. R., Rogers, R., Todd, J. D., Brearley, C. A. & Johnston, A. W. Molecular
891 genetic analysis of a dimethylsulfoniopropionate lyase that liberates the climate-
892 changing gas dimethylsulfide in several marine alpha-proteobacteria and *Rhodobacter*
893 *sphaeroides*. *Environ. Microbiol.* **10**, 757–767 (2008).
- 894 71. Todd, J. D., Curson, A. R. J., Dupont, C. L., Nicholson, P. & Johnston, A. W. B. The
895 dddP gene, encoding a novel enzyme that converts dimethylsulfoniopropionate into
896 dimethyl sulfide, is widespread in ocean metagenomes and marine bacteria and also
897 occurs in some Ascomycete fungi (vol 11, pg 1376, 2009). *Environ. Microbiol.* **11**,
898 1624–1625 (2009).
- 899 72. Todd, J. D. *et al.* DddQ, a novel, cupin-containing, dimethylsulfoniopropionate lyase
900 in marine roseobacters and in uncultured marine bacteria. *Environ. Microbiol.* **13**,
901 427–438 (2011).

- 902 73. Curson, A. R. J., Sullivan, M. J., Todd, J. D. & Johnston, A. W. B. DddY, a
903 periplasmic dimethylsulfoniopropionate lyase found in taxonomically diverse species
904 of Proteobacteria. *ISME J.* **5**, 1191–1200 (2011).
- 905 74. Todd, J. D., Kirkwood, M., Newton-Payne, S. & Johnston, A. W. B. DddW, a third
906 DMSP lyase in a model Roseobacter marine bacterium, *Ruegeria pomeroyi* DSS-3.
907 *ISME J.* **6**, 223–226 (2012).
- 908 75. Alcolombri, U. *et al.* Identification of the algal dimethyl sulfide-releasing enzyme: A
909 missing link in the marine sulfur cycle. *Science* (80-.). **348**, 1466–1469 (2015).
- 910 76. Eddy, S. R. Accelerated profile HMM searches. *PLoS Comput. Biol.* **7**, (2011).
- 911 77. Fish, J. A. *et al.* FunGene: the functional gene pipeline and repository. *Front.*
912 *Microbiol.* **4**, (2013).
- 913 78. Price, M. N., Dehal, P. S. & Arkin, A. P. FastTree 2 – approximately maximum-
914 likelihood trees for large alignments. *PLoS One* **5**, e9490 (2010).
- 915 79. Letunic, I. & Bork, P. Interactive tree of life (iTOL) v3: an online tool for the display
916 and annotation of phylogenetic and other trees. *Nucleic Acids Res.* **44**, (2016).
- 917 80. Masella, A. P., Bartram, A. K., Truszkowski, J. M., Brown, D. G. & Neufeld, J. D.
918 PANDAseq: PAired-eND Assembler for Illumina sequences. *BMC Bioinformatics* **13**,
919 (2012).

920 **Correspondence and requests for materials** should be addressed to Jonathan D. Todd
921 (jonathan.todd@uea.ac.uk).

922

923 **Acknowledgements** Funding from the Natural Environment Research Council
924 (NE/J01138X, NE/M004449, NE/N002385 and NE/P012671) supported work in J.D.T.'s
925 laboratory. We thank Pamela Wells and Marco Giardina for general technical support, and
926 Robert Green, Ji Liu and Colin Murrell for advice and discussion of results. We also
927 acknowledge the *Tara* Oceans Consortium for providing metagenomic sequence data, and the
928 facilities at the Australian Microscopy & Microanalysis Research Facility at the Centre for
929 Microscopy, Characterisation & Analysis, University of Western Australia, a facility funded
930 by the University, State and Commonwealth Governments. The NanoSIMS work was
931 supported by an Australian Research Council Grant DE160100636 to J-B.R.

932

933 **Author contributions** J.D.T. wrote the paper, designed experiments and performed
934 experiments (gene cloning, enzyme assays, bioinformatics) and analysed data; A.R.J.C. wrote
935 the paper, designed experiments, performed experiments (gene cloning, enzyme assays, gas
936 chromatography to quantify DMSP/DMSHB, phytoplankton growth experiments), analysed
937 data and prepared figures/tables; B.T.W. performed experiments (bioinformatics analysis of
938 DsyB/DSYB in transcriptomes, metagenomes and metatranscriptomes, phylogenetic tree
939 construction), analysed data and prepared figures/tables; B.J.P. performed experiments (gene
940 cloning, RNA isolation, qRT-PCR experiments, protein purification, *in vitro* enzyme assays
941 and Western Blots) and analysed data; L.P.S. performed experiments (gene cloning) and
942 analysed data; A.B.M. performed experiments (LC-MS detection of DMSP and glycine
943 betaine) and analysed data; P.L.R. performed experiments (phytoplankton growth
944 experiments); D.K. performed experiments (bioinformatic analysis and phylogenetic tree
945 construction); E.M. performed experiments (immunogold labelling, microscopy) and
946 prepared figures; L.G.S. wrote the paper, performed experiments (evolutionary analysis of

947 DsyB and DSYB sequences and phylogenetic tree construction) and prepared figures/tables;
948 J-B.R. wrote the paper, performed experiments (NanoSIMS, LC-MRM-MS) and prepared
949 figures; U.K. performed experiments (LC-MRM-MS); P.L.C. and P.G. performed
950 experiments (NanoSIMS); O.C. designed antibodies and prepared materials for microscopy;
951 S.M. performed experiments (bioinformatic analysis); R.A.C. supplied *C. tobin* CCMP291
952 strain. All authors reviewed the manuscript before submission.

953

954 **Competing interests**

955 The authors declare no competing financial interests.

956

957 **Additional Information**

958 **Supplementary Information** is linked to the online version of the paper.

959 **Reprints and permissions information** is available at www.nature.com/reprints.

960

961 **Figure legends**

962 **Figure 1. Transamination pathway for DMSP biosynthesis pathway in bacteria and**
963 **marine algae, and phylogenetic tree of DsyB/DSYB proteins**

964 **a**, Predicted pathway for DMSP biosynthesis in bacteria (*Labrenzia*), macroalgae (*Ulva*,
965 *Enteromorpha*), diatoms (*Thalassiosira*, *Melosira*), prymnesiophytes (*Emiliana*) and
966 prasinophytes (*Tetraselmis*). Abbreviations: Met, methionine; MTOB, 4-methylthio-2-
967 oxobutyrate; MTHB, 4-methylthio-2-hydroxybutyrate; DMSHB, 4-dimethylsulphonio-2-
968 hydroxybutyrate. **b**, Maximum likelihood phylogenetic tree of DsyB/DSYB proteins. Species
969 are colour-coded according to taxonomic class as shown in the key, with proteins shown to be
970 functional marked with an asterisk. Bootstrap support for nodes is marked. Based on 145
971 protein sequences.

972

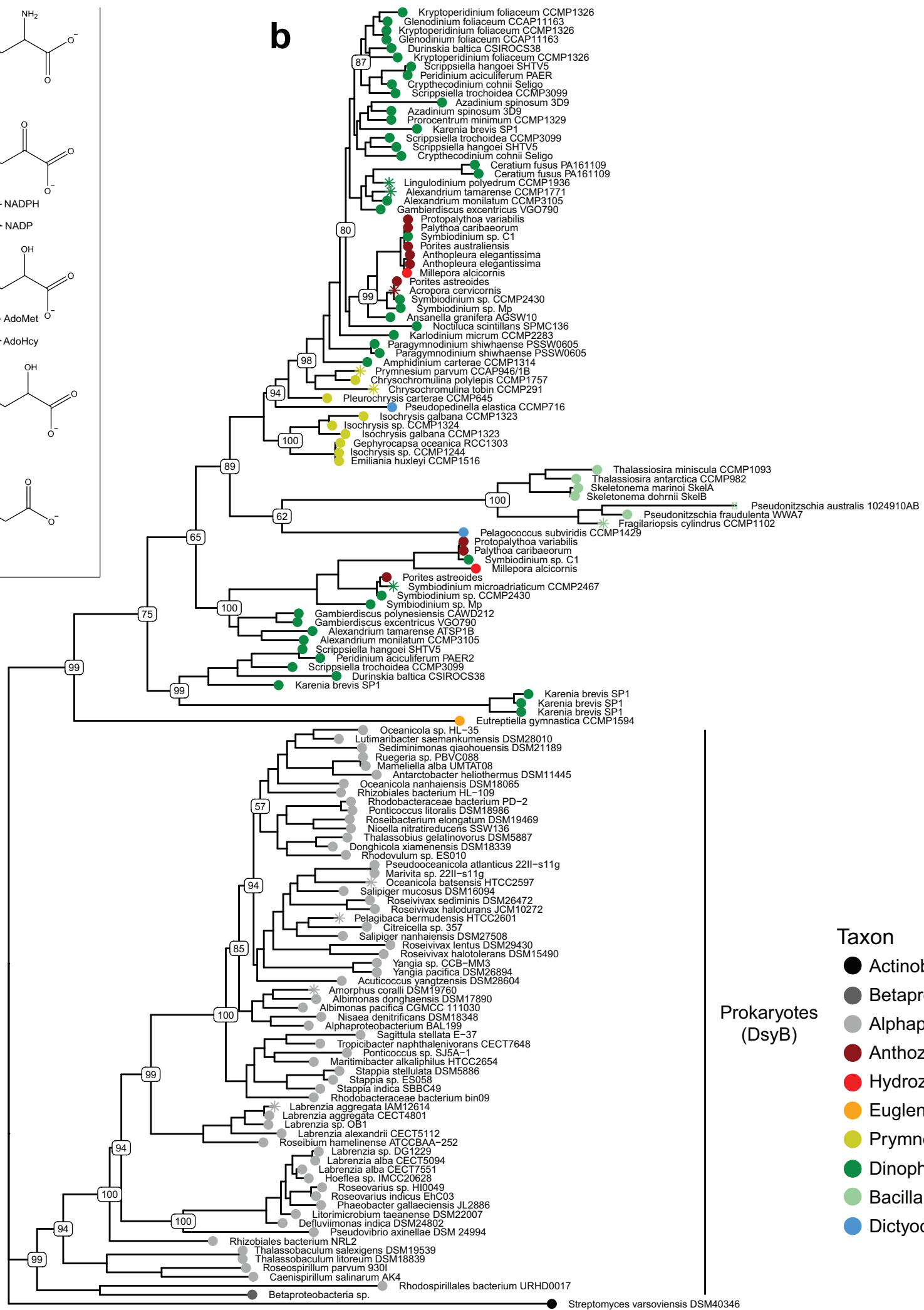
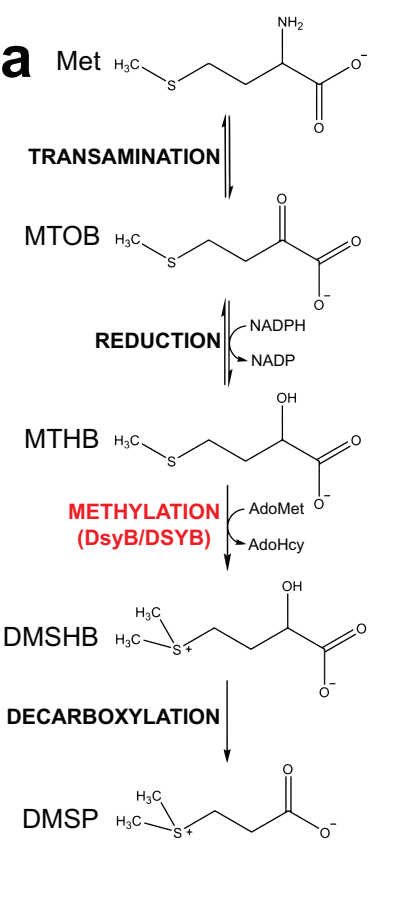
973 **Figure 2. Immunogold localisation of DSYB in *Prymnesium parvum* CCAP946/6**

974 Representative electron micrographs of *P. parvum* cells showing location of DSYB by
975 immunogold labelling. **a, b**, Immunostaining of cell with DSYB antibody and secondary
976 antibody with gold. **c, d**, Control immunostaining with pre-immune serum. **e, f**, Control
977 immunostaining with only secondary antibody. Boxes in **a, c**, and **e**, correspond to area
978 magnified in **b, d**, and **f** respectively. Scale bars are all 500 nm. Abbreviations: ch,
979 chloroplast; g, golgi apparatus; ig, immunogold; m, mitochondrion; nu, nucleus; py,
980 pyrenoid; ri, ribosome; v, vacuole. Experiments were repeated twice and two samples (n=2)
981 were used for each experiment.

982

983 **Figure 3. Sub-cellular distribution of ^{34}S in *Prymnesium parvum* CCAP946/6 following**
984 **sulfur uptake for 48 h. a-d**, Representative $^{12}\text{C}^{14}\text{N}/^{12}\text{C}_2$ mass images showing cellular
985 structures of *P. parvum* cells. The cells were imaged straight after the start of the incubation
986 (a), and after 6 h (b), 24 h (c) and 48 h (d). e-h, $^{34}\text{S}/^{32}\text{S}$ ratio of the same cells, shown as Hue
987 Saturation Intensity (HSI) images where the colour scale indicates the value of the $^{34}\text{S}/^{32}\text{S}$
988 ratio, with natural abundance in blue, changing to pink with increasing ^{34}S levels. Each image
989 was only acquired once. i, Isotope ratio of $^{34}\text{S}/^{32}\text{S}$ in different cellular regions (biological
990 replicates, number of cells analysed: T0: whole cells n = 7, chloroplasts n = 3, hotspot n = 10;
991 T6: whole cells n = 14, chloroplasts n = 6, hotspot n = 10; T24: whole cells n = 12,
992 chloroplasts n = 9, hotspot n = 10; and T48: whole cells n = 6, chloroplasts n = 4, hotspot n =
993 10; error bars are shown for standard error). Abbreviations, ch: chloroplast; h: hotspot; py:
994 pyrenoid; v: vacuole. Scale bars: 1 μm .

995



Taxon

- Actinobacteria
- Betaproteobacteria
- Alphaproteobacteria
- Anthozoa
- Hydrozoa
- Euglenophyceae
- Prymnesiophyceae
- Dinophyceae
- Bacillariophyceae
- Dictyochophyceae

